Supporting Information

Appendix S1

Remote sensing of temperature-dependent mosquito and viral traits predicts field surveillance-based disease risk

Andrew J. MacDonald, David Hyon, Samantha Sambado, Kacie Ring, Anna Boser

Ecology

Figure S1.
Temperature-dependent mosquito abundance, M(T). Predictions represent average trait values calculated from air temperature raster images from ECOSTRESS from across the diurnal cycle during the summer months when West Nile virus and mosquito abundance peak[1].

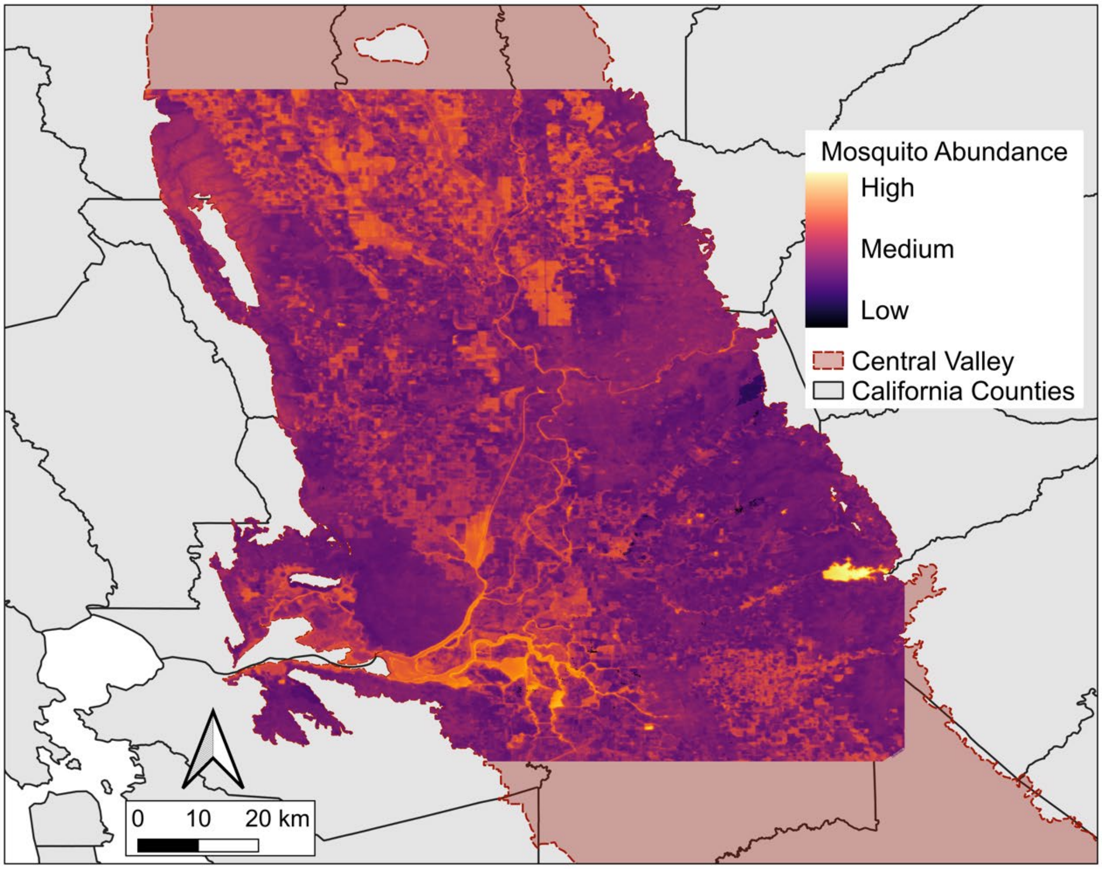

Figure S2.
Temperature-dependent transmission efficiency, b(T). Predictions represent average trait values calculated from air temperature raster images from ECOSTRESS from across the diurnal cycle during the summer months when West Nile virus and mosquito abundance peak[1].

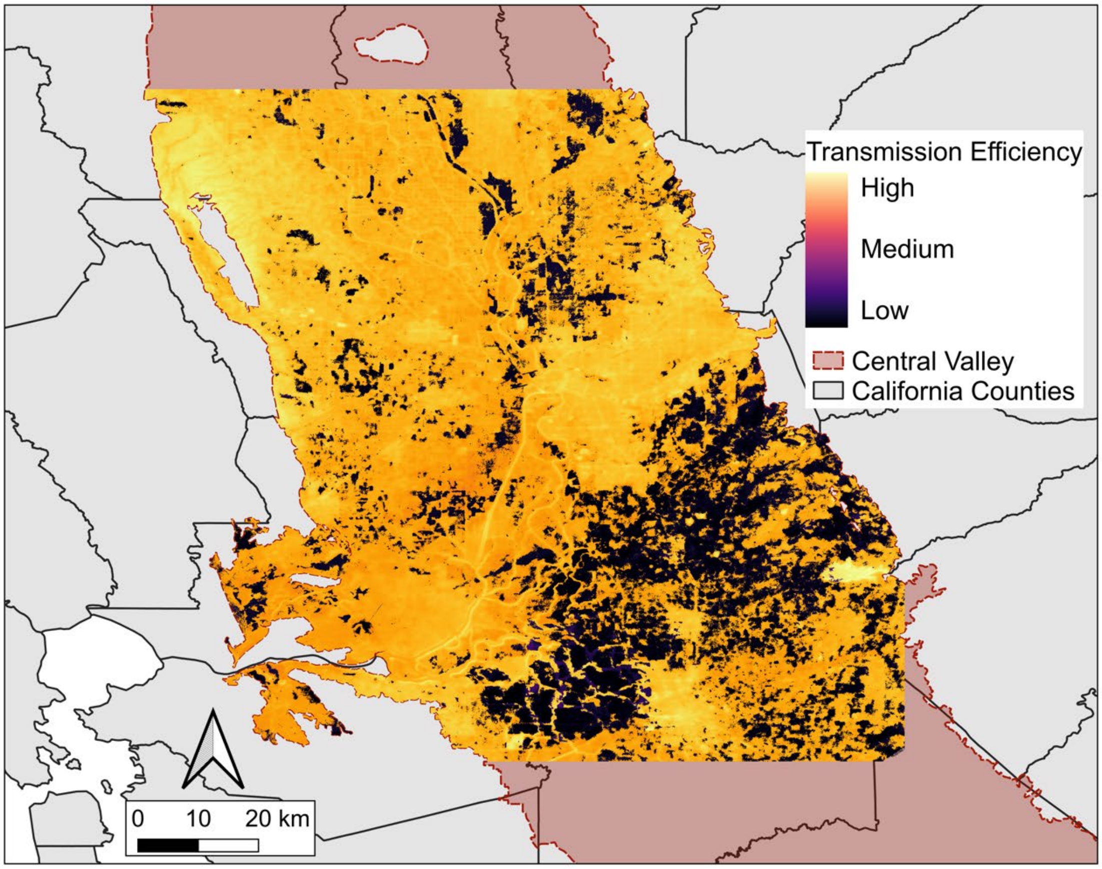

Figure S3.
Results of spatial thinning of trap station clusters to remove effects of spatial autocorrelation[2]. Panel a) trap station clusters prior to spatial thinning, panel b) trap station clusters following spatial thinning; color represents unique cluster ID's. Clusters in the northeastern region of the plots, from around Lake Tahoe, CA, were dropped when restricting the data to the Central Valley.

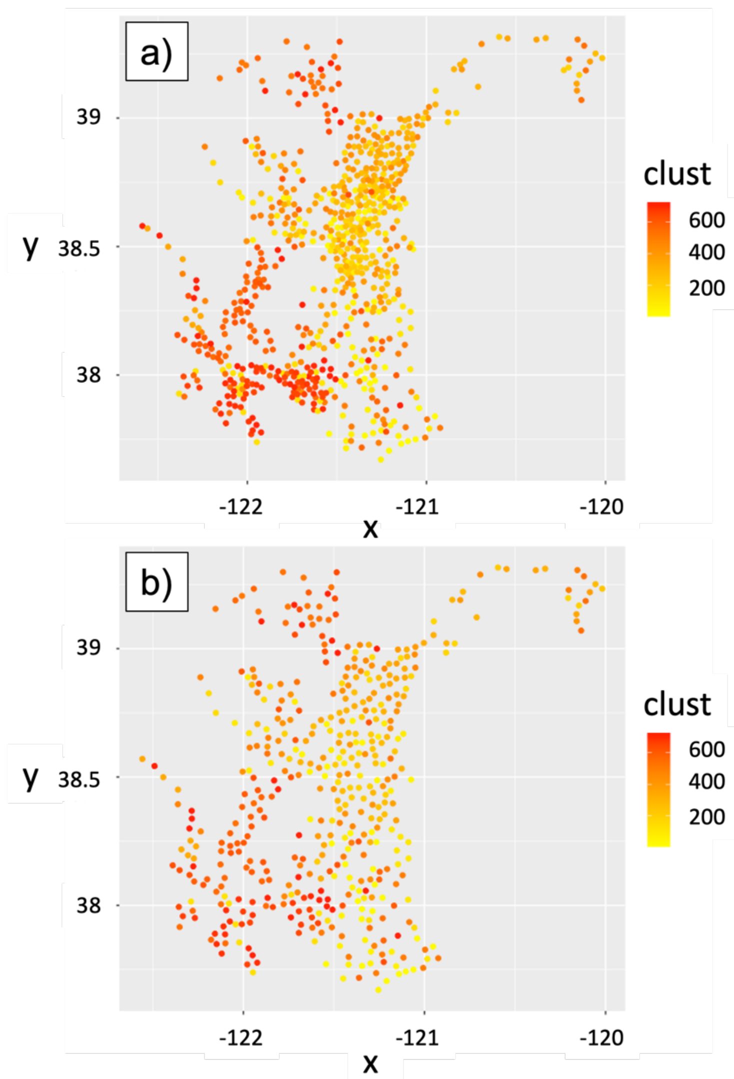

Figure S4.
Model diagnostic plots from the DHARMa package[3] for best fit model (raw mosquitos/trap night as outcome, predicted by temperature-dependent mosquito abundance):

Test of overdispersion:

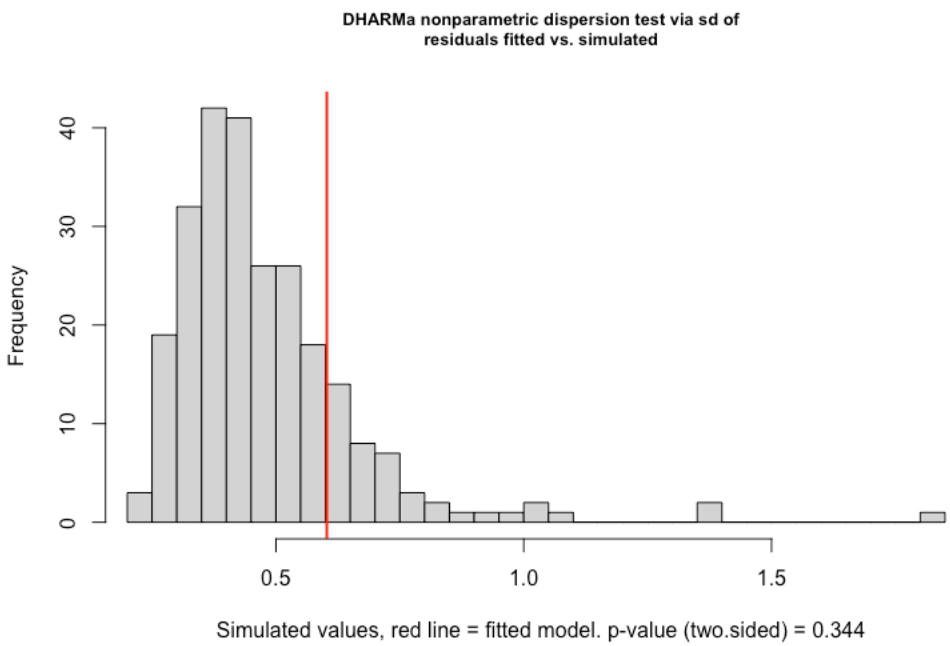

QQ plot and residual vs. predicted:

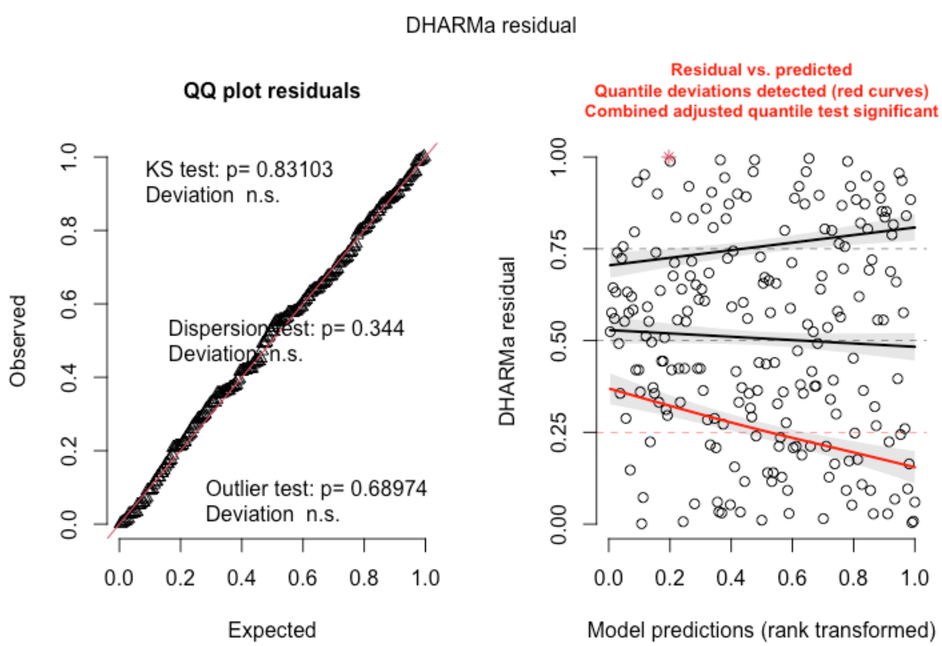

Moran's I test of spatial autocorrelation on best fit model residuals: observed = 0.0034, expected = -0.0047, sd=0.0068, p=0.23. The plot illustrates no spatial pattern in residuals, with points representing residuals plotted in x, y space, with a gradient of dark blue to dark red representing the magnitude and sign of residuals.

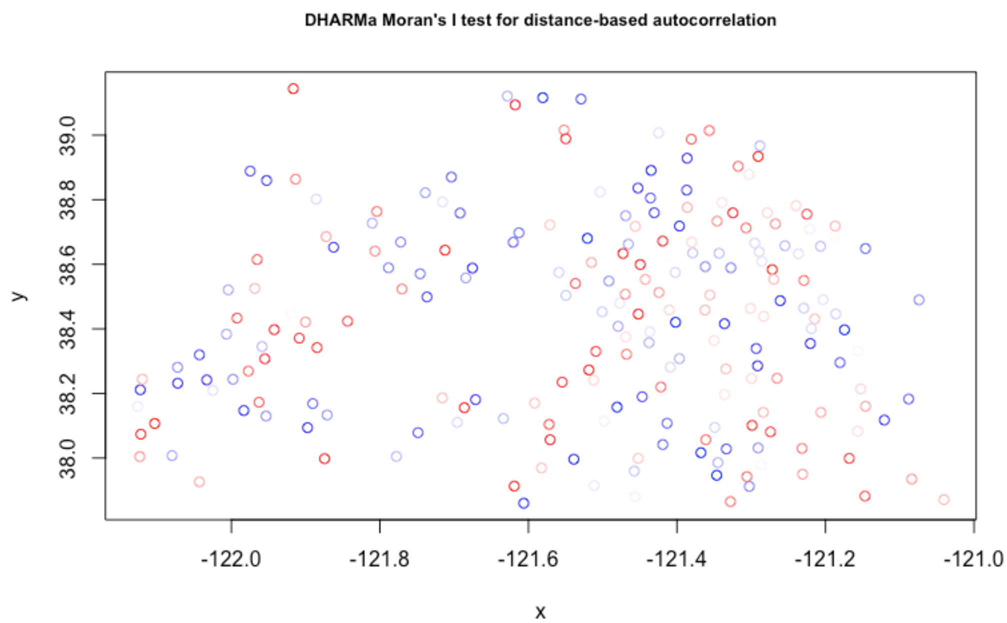

VIF table for best fit model: produced using the check_collinearity() function in the performance package[4].

Low Correlation

Term	VIF	VIF 95% CI	Increased SE	Tolerance	Tolerance 95% CI
competent_bird_abundance.mean_std	2.91	[2.40, 3.60]	1.71	0.34	[0.28, 0.42]
Mean_Bird_Diversity.mean_std	2.20	[1.85, 2.69]	1.48	0.46	[0.37, 0.54]
GRIDMET_Precip_mm.mean_std	4.05	[3.29, 5.05]	2.01	0.25	[0.20, 0.30]
VPD_kPa.mean_std	3.46	[2.83, 4.30]	1.86	0.29	[0.23, 0.35]
jrcStandingWater.mean_std	4.01	[3.27, 5.01]	2.00	0.25	[0.20, 0.31]
xcoord_scale	4.48	[3.63, 5.61]	2.12	0.22	[0.18, 0.28]

Moderate Correlation

Term	VIF	VIF 95% CI	Increased SE	Tolerance	Tolerance 95% CI
abund_mean_std	6.00	[4.82, 7.55]	2.45	0.17	[0.13, 0.21]
irrWater.mean_std	9.70	[7.71, 12.27]	3.11	0.10	[0.08, 0.13]
EVI.mean_std	6.90	[5.52, 8.69]	2.63	0.14	[0.12, 0.18]
Cattl_mean_std	5.27	[4.25, 6.61]	2.30	0.19	[0.15, 0.24]
NLCD_majority2	9.29	[7.40, 11.75]	3.05	0.11	[0.09, 0.14]
ycoord_scale	6.51	[5.22, 8.20]	2.55	0.15	[0.12, 0.19]

Figure S5.
Model diagnostic plots from the DHARMa package[3] for best fit model (raw minimum infection rate as outcome, predicted by temperature-dependent transmission efficiency):
Test of overdispersion:

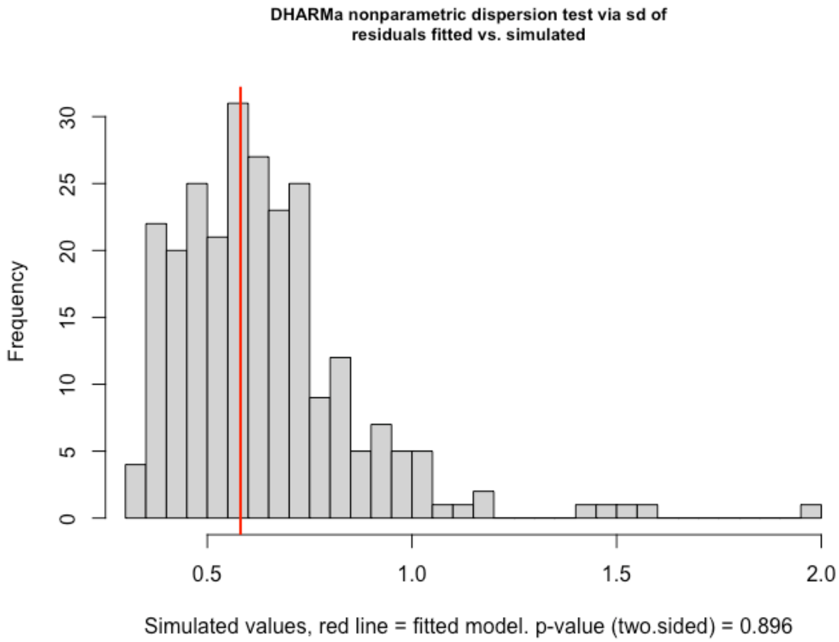

QQ plot and residual vs. predicted:

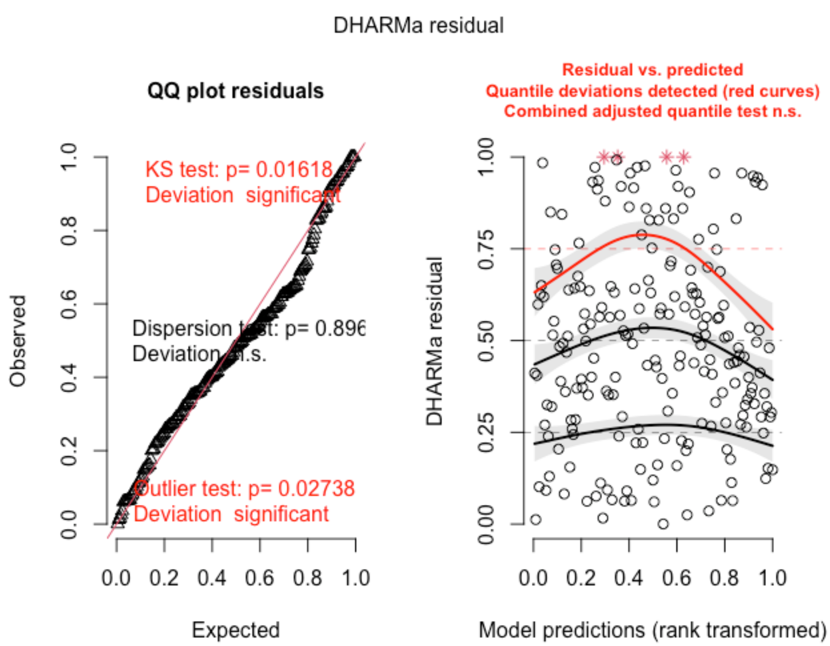

Moran's I test of spatial autocorrelation on best fit model residuals: observed = 0.0042, expected = -0.0048, sd=0.007, p=0.2. The plot illustrates no spatial pattern in residuals, with points representing residuals plotted in x, y space, with a gradient of dark blue to dark red representing the magnitude and sign of residuals.

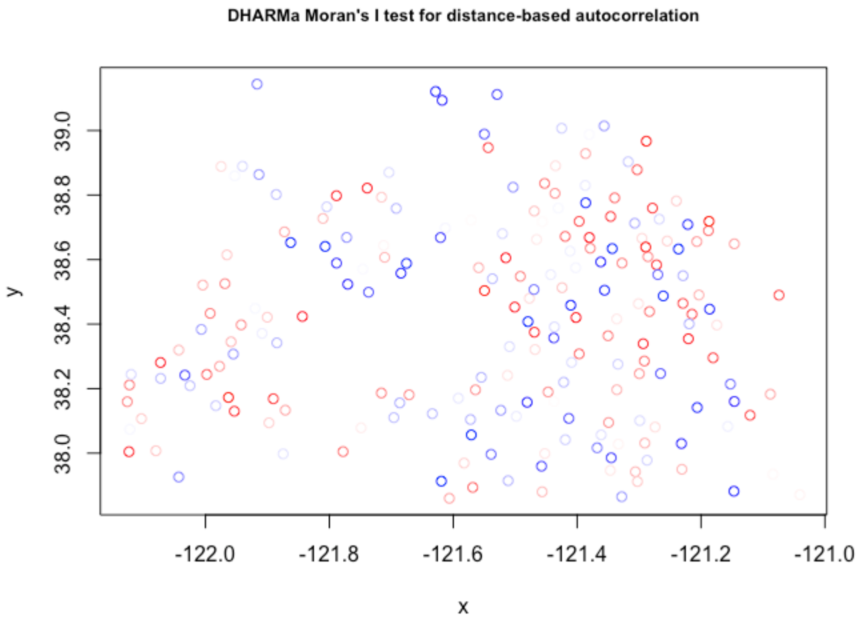

VIF table for best fit model: produced using the check_collinearity() function in the performance package[4].

Low Correlation

Term	VIF	VIF 95% CI	Increased SE	Tolerance	Tolerance 95% CI
trans_mean_std	3.80	[3.09, 4.75]	1.95	0.26	[0.21, 0.32]
Mean_Bird_Diversity.mean_std	1.97	[1.67, 2.41]	1.40	0.51	[0.41, 0.60]
EVI.mean_std	3.40	[2.78, 4.24]	1.85	0.29	[0.24, 0.36]
VPD_kPa.mean_std	1.95	[1.65, 2.39]	1.40	0.51	[0.42, 0.60]
bite_mean_std	4.09	[3.32, 5.13]	2.02	0.24	[0.19, 0.30]
jrcStandingWater.mean_std	3.74	[3.04, 4.67]	1.93	0.27	[0.21, 0.33]
CApop_mean_std	3.69	[3.00, 4.61]	1.92	0.27	[0.22, 0.33]
Chick_mean_std	4.45	[3.60, 5.59]	2.11	0.22	[0.18, 0.28]
ycoord_scale	2.45	[2.04, 3.02]	1.56	0.41	[0.33, 0.49]
NLCD_majority2	7.68	[6.12, 9.72]	2.77	0.13	[0.10, 0.16]

Moderate Correlation

Term	VIF	VIF 95% CI	Increased SE	Tolerance	Tolerance 95% CI
xcoord_scale	2.51	[2.08, 3.09]	1.58	0.40	[0.32, 0.48]

Figure S6.
Model diagnostic plots from the DHARMa package[3] for best fit model (raw minimum infection rate as outcome, predicted by air temperature):

Test of overdispersion:

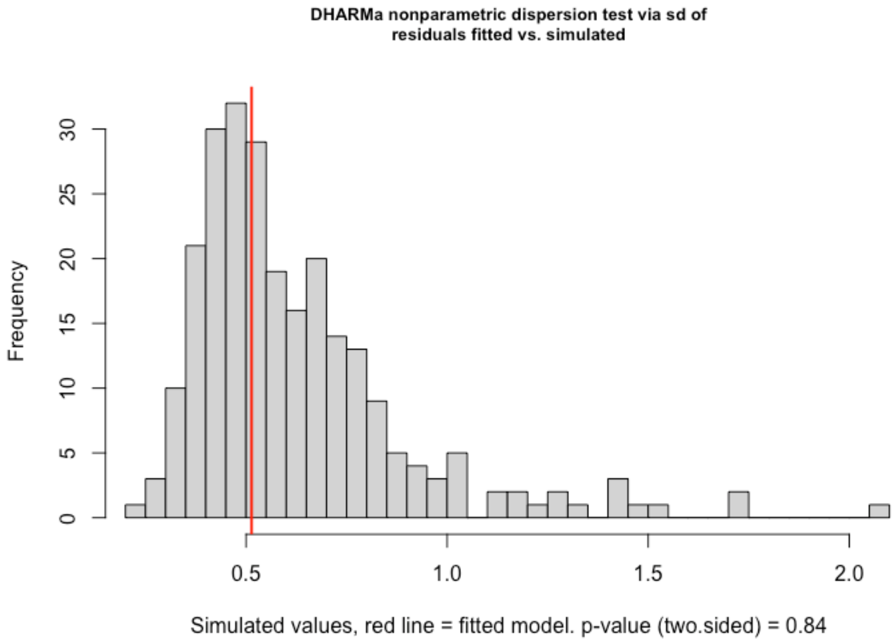

QQ plot and residual vs. predicted:

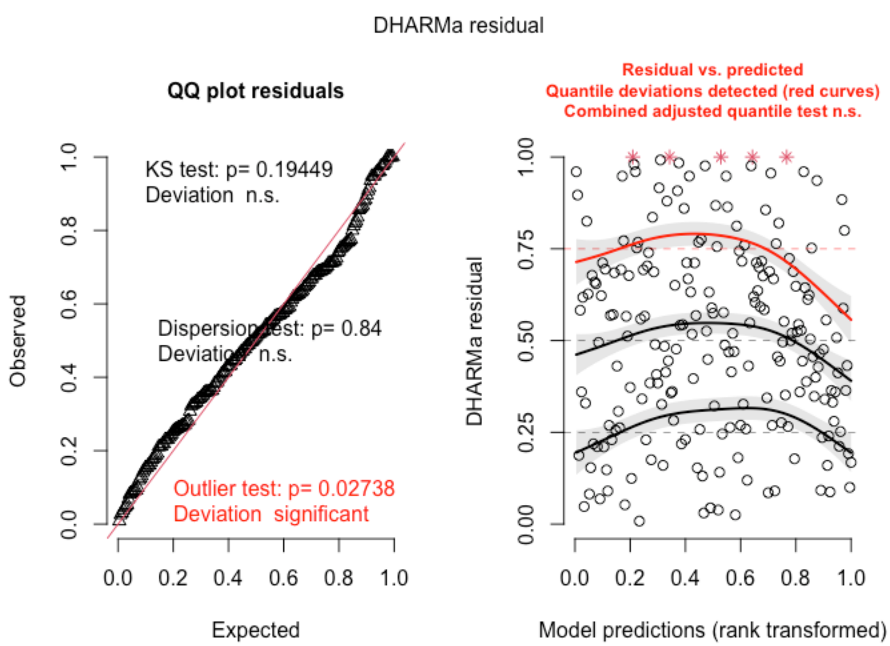

Moran's I test of spatial autocorrelation on best fit model residuals: observed = 0.0055, expected = -0.0048, sd=0.007, p=0.14. The plot illustrates no spatial pattern in residuals, with points representing residuals plotted in x, y space, with a gradient of dark blue to dark red representing the magnitude and sign of residuals.

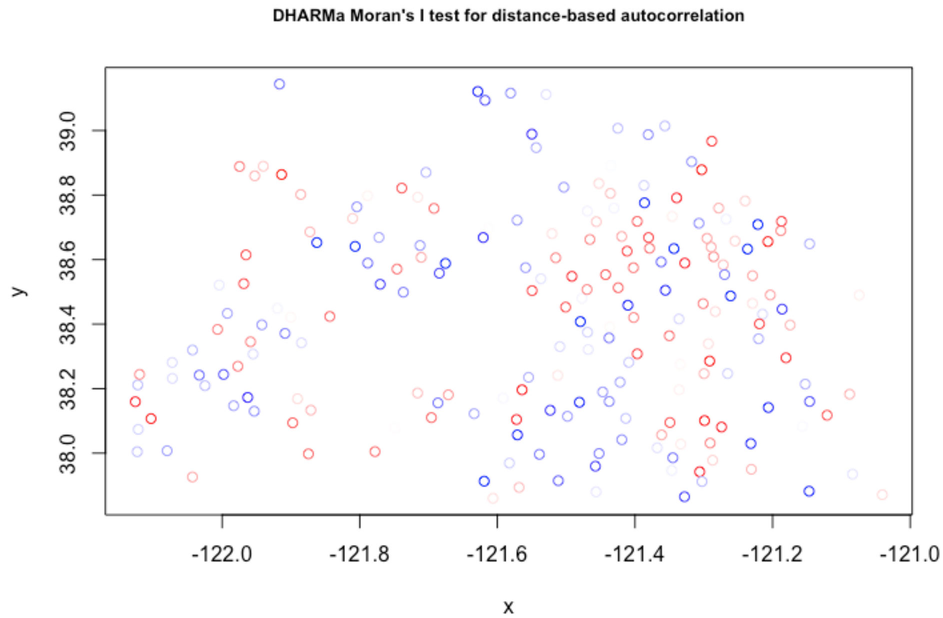

VIF table for best fit model: produced using the check_collinearity() function in the performance package[4].

Low Correlation

Term	VIF	VIF 95% CI	Increased SE	Tolerance	Tolerance 95% CI
airT_mean_std	4.44	[3.58, 5.60]	2.11	0.23	[0.18, 0.28]
I(airT_mean_std^2)	1.19	[1.08, 1.48]	1.09	0.84	[0.68, 0.93]
amerob_abundance.mean_std	1.86	[1.58, 2.29]	1.36	0.54	[0.44, 0.63]
houspa_abundance.mean_std	1.86	[1.58, 2.28]	1.36	0.54	[0.44, 0.63]
cowscj_abundance.mean_std	4.28	[3.45, 5.40]	2.07	0.23	[0.19, 0.29]
Mean_Bird_Diversity.mean_std	2.17	[1.82, 2.68]	1.47	0.46	[0.37, 0.55]
EVI.mean_std	3.40	[2.77, 4.26]	1.84	0.29	[0.23, 0.36]
CApop_mean_std	2.92	[2.40, 3.64]	1.71	0.34	[0.27, 0.42]
Chick_mean_std	1.75	[1.49, 2.14]	1.32	0.57	[0.47, 0.67]

Table S1. Summary of data sources for each methods section with respective hyperlinks and references (below). All data were summarized within the region of interest in the northern Central Valley using the polygon files archived on Zenodo ("Northern_Central_Valley.shp" and "trap_clusters.shp" polygons)[5]. To obtain surveillance data, a data request to CalSurv would include the following parameters: All trap types, all *Culex* species mosquitos, West Nile virus mosquito pools, for 2018 through 2020 in Sacramento, Solano, Napa, Yolo, Colusa, Sutter, Placer, Yuba, Nevada, Contra Costa, San Joaquin, El Dorado, and Amador Counties. Final processed dataset and code to replicate analyses and results have been archived on Zenodo[5].

METHODS SECTION	DATA	SOURCE	HYPERLINK
WNV surveillance data	Mosquito abundance (*Culex tarsalis* females)	VectorSurv, CalSurv data request	https://gateway.vectorsurv.org/ https://vectorsurv.org/assets/files/calsurv_data_policy.pdf
	WNV MIR (calculated for *Culex tarsalis* females)	VectorSurv, CalSurv data request	https://gateway.vectorsurv.org/ https://vectorsurv.org/assets/files/calsurv_data_policy.pdf
Temperature-dependent traits	LST at 70 m: all cloud free images between 04/01 and 9/30 from the years 2018-2021, using the Northern_Central_Valley.shp polygon for the APPEEARS data request, and averaged within the trap_clusters.shp polygon. The data processing workflow and methods are described in detail in Boser et al. 2021[1].	ECOSTRESS[6]	https://appeears.earthdatacloud.nasa.gov/
Abiotic and biotic controls	Bird abundance: median abundance estimates from ebird status and trends for western scrub jays, American robins, American crows, house finches and house sparrows (and the sum of all target species) between 4/15 and 9/30 of 2019, averaged within the trap_clusters.shp polygon.	eBird[7]	https://science.ebird.org/en/status-and-trends/download-data
	Shannon's Diversity calculated per raster cell using median abundance of all birds in the data file "caSpeciesList.txt" archived on Zenodo[5] between 4/15 and 9/30 of 2019, averaged within the trap_clusters.shp polygon.		
	Human density: annual population estimate from	WorldPop[8]	https://hub.worldpop.org/project/categories?id=3

2017, averaged within the trap_clusters.shp polygon.		
Cattle/chicken density: annual density estimate from 2015, averaged within the trap_clusters.shp polygon.	UN FAO[9]	https://data.apps.fao.org/catalog/dataset/glw/resource/23610e26-4f8c-4f1d-9b61-fbe1f5fcb807
EVI: raster images between 06/01 and 9/30 from the years 2018-2020, averaged within the trap_clusters.shp polygon.	MODIS[10]	https://developers.google.com/earth-engine/datasets/catalog/MODIS_061_MOD13A2
Precipitation, vapor pressure deficit: raster images between 06/01 and 9/30 from the years 2018-2020, averaged within the trap_clusters.shp polygon.	gridMET[11]	https://www.drought.gov/data-maps-tools/gridded-surface-meteorological-gridmet-dataset
Palmer drought severity index: raster images between 06/01 and 9/30 from the years 2018-2020, averaged within the trap_clusters.shp polygon.	gridMET[11]	https://www.drought.gov/data-maps-tools/us-gridded-palmer-drought-severity-index-pdsi-gridmet
Area of irrigated agriculture: annual raster images from the years 2018-2020, averaged within the trap_clusters.shp polygon.	IrrMapper[12]	https://doi.org/10.3390/rs12142328
Standing water: raster images between 06/01 and 9/30 from the years 2018-2020, averaged within the trap_clusters.shp polygon.	JRC[13]	https://global-surface-water.appspot.com/
Land cover class: dominant (mode) land cover class (of natural vegetation, wetlands, agriculture, and developed) within each trap_clusters.shp polygon.	NLCD[14]	https://www.usgs.gov/node/279743

Table S2.
Table of base model and full model regression results (raw mosquitos/trap night as outcome, predicted by temperature-dependent mosquito abundance).

	Mos. per Trap Night			
Predictors	*Estimates*	*CI*	*Estimates*	*CI*
(Intercept)	16.04	13.48 – 19.10	13.07	8.25 – 20.70
Temp-Dependent Mos. Abundance	1.37	1.13 – 1.67	1.46	1.03 – 2.06
Competent Bird Host Abundance			1.76	1.30 – 2.37
Bird Diversity			0.60	0.50 – 0.72
Precip. (mm)			2.01	0.98 – 4.13
Irrigated Ag. Area			1.49	0.95 – 2.32
PDSI Drought			0.95	0.71 – 1.28
Enhanced Vegetation Index			0.46	0.31 – 0.71
Vapor Pressure Deficit			0.59	0.37 – 0.93
Area of Standing Water			0.64	0.47 – 0.88
Human Population Density			0.90	0.68 – 1.19
Cattle Density			1.32	0.87 – 1.98
Chicken Density			1.02	0.72 – 1.45
Land Cover, Developed			0.24	0.12 – 0.47
Land Cover, Natural			0.73	0.40 – 1.33
Land Cover, Wetland			4.99	1.85 – 13.52
x coordinate			0.53	0.37 – 0.78
y coordinate			1.58	1.17 – 2.15
Observations	214		214	
R^2 conditional / R^2 marginal	NA / 0.158		NA / 0.804	

Table S3.
Table of best fit model results (raw mosquitos/trap night as outcome, predicted by temperature-dependent mosquito abundance).

	Mos. per Trap Night	
Predictors	*Estimates*	*CI*
(Intercept)	13.63	9.19 – 20.22
Temp-Dependent Mos. Abundance	1.42	1.02 – 1.97
Competent Bird Host Abundance	1.70	1.28 – 2.27
Bird Diversity	0.61	0.51 – 0.72
Precip. (mm)	1.97	1.04 – 3.72
Irrigated Ag. Area	1.57	1.03 – 2.38
Enhanced Vegetation Index	0.47	0.31 – 0.70
Vapor Pressure Deficit	0.58	0.37 – 0.91
Area of Standing Water	0.66	0.48 – 0.90
Cattle Density	1.35	0.97 – 1.88
Land Cover, Developed	0.21	0.12 – 0.37
Land Cover, Natural	0.75	0.41 – 1.35
Land Cover, Wetland	5.20	2.00 – 13.54
x coordinate	0.53	0.40 – 0.70
y coordinate	1.56	1.17 – 2.09
Observations	214	
R^2 conditional / R^2 marginal	NA / 0.803	

Table S4.
Table of full and best fit model results using all model comparison for model selection using the dredge function in the MuMIn package[15] (raw mosquitos/trap night as outcome, predicted by temperature-dependent mosquito abundance). The determination of best fit model does not change with this alternative model selection approach.

	Mos. per Trap Night			
Predictors	*Estimates*	*CI*	*Estimates*	*CI*
(Intercept)	13.07	8.25 – 20.70	13.63	9.19 – 20.22
Temp-Dependent Mos. Abundance	1.46	1.03 – 2.06	1.42	1.02 – 1.97
Competent Bird Host Abundance	1.76	1.30 – 2.37	1.70	1.28 – 2.27
Bird Diversity	0.60	0.50 – 0.72	0.61	0.51 – 0.72
Precip. (mm)	2.01	0.98 – 4.13	1.97	1.04 – 3.72
Irrigated Ag. Area	1.49	0.95 – 2.32	1.57	1.03 – 2.38
PDSI Drought	0.95	0.71 – 1.28		
Enhanced Vegetation Index	0.46	0.31 – 0.71	0.47	0.31 – 0.70
Vapor Pressure Deficit	0.59	0.37 – 0.93	0.58	0.37 – 0.91
Area of Standing Water	0.64	0.47 – 0.88	0.66	0.48 – 0.90
Human Population Density	0.90	0.68 – 1.19		
Cattle Density	1.32	0.87 – 1.98	1.35	0.97 – 1.88
Chicken Density	1.02	0.72 – 1.45		
Land Cover, Developed	0.24	0.12 – 0.47	0.21	0.12 – 0.37
Land Cover, Natural	0.73	0.40 – 1.33	0.75	0.41 – 1.35
Land Cover, Wetland	4.99	1.85 – 13.52	5.20	2.00 – 13.54
x coordinate	0.53	0.37 – 0.78	0.53	0.40 – 0.70
y coordinate	1.58	1.17 – 2.15	1.56	1.17 – 2.09
Observations	214		214	
R^2 conditional / R^2 marginal	NA / 0.804		NA / 0.803	

Table S5.
Table of base model and full model regression results (raw minimum infection rate as outcome, predicted by temperature-dependent transmission efficiency):

	WNV MIR			
Predictors	*Estimates*	*CI*	*Estimates*	*CI*
(Intercept)	1.62	1.25 – 2.10	0.45	0.19 – 1.09
Transmission Efficiency	0.93	0.70 – 1.22	1.61	0.98 – 2.65
American Crow Abundance			0.76	0.43 – 1.34
American Robin Abundance			0.73	0.44 – 1.20
House Finch Abundance			1.08	0.52 – 2.28
House Sparrow Abundance			1.36	0.79 – 2.32
Scrub Jay Abundance			1.75	0.99 – 3.09
Bird Diversity			1.43	0.90 – 2.26
Precip. (mm)			0.63	0.26 – 1.55
Irrigated Ag. Area			1.18	0.50 – 2.79
PDSI Drought			1.54	0.93 – 2.56
Enhanced Vegetation Index			1.59	0.73 – 3.44
Vapor Pressure Deficit			1.80	0.55 – 5.92
Mosquito Biting Rate			0.31	0.09 – 1.00
Temp-Dependent Mosquito Abundance			1.18	0.42 – 3.27
Area of Standing Water			2.56	0.87 – 7.47
Human Population Density			0.48	0.27 – 0.88
Cattle Density			1.46	0.87 – 2.45
Chicken Density			1.61	0.92 – 2.80
Land Cover, Developed			2.49	0.68 – 9.09
Land Cover, Natural			0.59	0.20 – 1.79
Land Cover, Wetland			0.00	0.00 – Inf
Observations	210		210	
R^2 conditional / R^2 marginal	NA / 0.007		NA / 0.985	

Table S6.
Table of best fit model results (raw minimum infection rate as outcome, predicted by temperature-dependent transmission efficiency). Wetland land cover is relatively rare in the dataset (n=7 observations have wetland as dominant land cover) and all observations with wetland land cover have estimated MIR of 0. This inflates the coefficient estimate/confidence interval on wetland land cover. Removing the NLCD variable, however, has little effect on the estimated coefficients on the other variables, so we decide to retain NLCD in the best fit model.

	WNV MIR	
Predictors	*Estimates*	*CI*
(Intercept)	0.60	0.29 – 1.23
Transmission Efficiency	1.84	1.14 – 2.95
Bird Diversity	1.53	1.11 – 2.12
Enhanced Vegetation Index	1.93	1.19 – 3.12
Vapor Pressure Deficit	1.69	0.59 – 4.83
Mosquito Biting Rate	0.30	0.14 – 0.64
Area of Standing Water	2.30	0.82 – 6.46
Human Population Density	0.56	0.33 – 0.93
Chicken Density	1.38	0.87 – 2.19
Land Cover, Developed	2.47	0.82 – 7.44
Land Cover, Natural	0.53	0.20 – 1.41
Land Cover, Wetland	0.00	0.00 – Inf
x coordinate	1.52	0.98 – 2.36
y coordinate	0.90	0.65 – 1.25
Observations	210	
R^2 conditional / R^2 marginal	NA / 0.985	

Table S7.
Table of full and best fit model results using all model comparison for model selection using the dredge function in the MuMIn package[15] (raw minimum infection rate as outcome, predicted by temperature-dependent transmission efficiency). The full model had to be simplified, by replacing individual bird species abundances with a composite metric of abundance for all species combined, due to model convergence issues among the set of models being compared using all possible model comparison. The determination of best fit model does not change with this alternative model selection approach.

	WNV MIR			
Predictors	*Estimates*	*CI*	*Estimates*	*CI*
(Intercept)	0.50	0.21 – 1.18	0.60	0.29 – 1.23
Transmission Efficiency	1.73	1.07 – 2.80	1.84	1.14 – 2.95
Competent Bird Abundance	1.07	0.62 – 1.84		
Bird Diversity	1.60	1.15 – 2.25	1.53	1.11 – 2.12
Precip. (mm)	0.71	0.32 – 1.59		
Irrigated Ag. Area	0.92	0.41 – 2.06		
PDSI Drought	1.52	0.92 – 2.54		
Enhanced Vegetation Index	2.08	1.02 – 4.25	1.93	1.19 – 3.12
Vapor Pressure Deficit	2.51	0.81 – 7.78	1.69	0.59 – 4.83
Mosquito Biting Rate	0.33	0.11 – 0.96	0.30	0.14 – 0.64
Temp-Dependent Mosquito Abundance	0.95	0.36 – 2.49		
Area of Standing Water	2.89	1.02 – 8.17	2.30	0.82 – 6.46
Human Population Density	0.55	0.31 – 0.97	0.56	0.33 – 0.93
Cattle Density	1.41	0.86 – 2.30		
Chicken Density	1.58	0.92 – 2.71	1.38	0.87 – 2.19
Land Cover, Developed	2.56	0.73 – 9.03	2.47	0.82 – 7.44
Land Cover, Natural	0.56	0.19 – 1.67	0.53	0.20 – 1.41
Land Cover, Wetland	0.00	0.00 – Inf	0.00	0.00 – Inf
x coordinate			1.52	0.98 – 2.36
y coordinate			0.90	0.65 – 1.25
Observations	210		210	
R^2 conditional / R^2 marginal	NA / 0.985		NA / 0.985	

Table S8.
Table of best fit model results (raw minimum infection rate as outcome, predicted by air temperature).

	WNV MIR	
Predictors	*Estimates*	*CI*
(Intercept)	1.04	0.65 – 1.68
Air Temp (C)	2.12	0.98 – 4.62
Air Temp sq. (C)	0.64	0.38 – 1.06
American Robin Abundance	0.56	0.36 – 0.86
House Sparrow Abundance	1.36	0.93 – 1.99
Scrub Jay Abundance	1.47	0.87 – 2.50
Bird Diversity	1.48	1.02 – 2.16
Enhanced Vegetation Index	2.00	1.22 – 3.28
Human Population Density	0.63	0.39 – 1.00
Chicken Density	1.80	1.34 – 2.42
Observations	210	
R^2 conditional / R^2 marginal	NA / 0.572	

Table S9.
Table of best fit model results (standardized minimum infection rate as outcome, predicted by air temperature).

	WNV MIR	
Predictors	*Estimates*	*CI*
(Intercept)	0.06	0.03 – 0.13
Air Temp (C)	2.06	0.49 – 8.58
Air Temp sq. (C)	0.30	0.12 – 0.78
American Robin Abundance	0.58	0.25 – 1.33
House Sparrow Abundance	1.89	0.90 – 3.96
Scrub Jay Abundance	1.52	0.55 – 4.20
Bird Diversity	3.68	1.15 – 11.81
Enhanced Vegetation Index	1.90	0.80 – 4.53
Human Population Density	0.59	0.28 – 1.24
Chicken Density	1.87	1.09 – 3.21
Observations	210	
R^2 conditional / R^2 marginal	NA / 0.697	

References:

1. Boser, A., D. Sousa, A. Larsen, and A. MacDonald. 2021. Micro-climate to macro-risk: mapping fine scale differences in mosquito-borne disease risk using remote sensing. *Environmental Research Letters* 16:124014.
2. Kindt, R., and R. Coe. 2005. Tree diversity analysis. A manual and software for common statistical methods for ecological and biodiversity studies.
3. Hartig F (2022). DHARMa: Residual Diagnostics for Hierarchical (Multi-Level / Mixed) Regression Models. R package version 0.4.6, <https://CRAN.R-project.org/package=DHARMa>.
4. Lüdecke, D., M. Ben-Shachar, I. Patil, P. Waggoner, and D. Makowski. 2021. performance: An R Package for Assessment, Comparison and Testing of Statistical Models. Journal of Open Source Software 6:3139.
5. MacDonald, A. J. 2024. Data and code for: Remote sensing of temperature-dependent mosquito and viral traits predicts field surveillance-based disease risk. https://doi.org/10.5281/zenodo.13344415
6. Fisher, J. B., B. Lee, A. J. Purdy, G. H. Halverson, M. B. Dohlen, K. Cawse-Nicholson, A. Wang, R. G. Anderson, B. Aragon, M. A. Arain, D. D. Baldocchi, J. M. Baker, H. Barral, C. J. Bernacchi, C. Bernhofer, S. C. Biraud, G. Bohrer, N. Brunsell, B. Cappelaere, S. Castro-Contreras, J. Chun, B. J. Conrad, E. Cremonese, J. Demarty, A. R. Desai, A. De Ligne, L. Foltýnová, M. L. Goulden, T. J. Griffis, T. Grünwald, M. S. Johnson, M. Kang, D. Kelbe, N. Kowalska, J. Lim, I. Maïnassara, M. F. McCabe, J. E. C. Missik, B. P. Mohanty, C. E. Moore, L. Morillas, R. Morrison, J. W. Munger, G. Posse, A. D. Richardson, E. S. Russell, Y. Ryu, A. Sanchez-Azofeifa, M. Schmidt, E. Schwartz, I. Sharp, L. Šigut, Y. Tang, G. Hulley, M. Anderson, C. Hain, A. French, E. Wood, and S. Hook. 2020. ECOSTRESS: NASA's next generation mission to measure evapotranspiration from the International Space Station. *Water Resources Research* 56:e2019WR026058.
7. Fink, D., T. Auer, A. Johnston, M. Strimas-Mackey, O. Robinson, S. Ligocki, W. Hochachka, C. Wood, I. Davies, M. Iliff, and L. Seitz. 2020. eBird Status and Trends, Data Version: 2019.
8. WorldPop: Open spatial demographic data and research. www.worldpop.org.
9. Gilbert, M., G. Nicolas, G. Cinardi, T. P. Van Boeckel, S. O. Vanwambeke, G. R. W. Wint, and T. P. Robinson. 2018. Global distribution data for cattle, buffaloes, horses, sheep, goats, pigs, chickens and ducks in 2010. *Scientific Data* 5:180227.
10. MODIS Terra Vegetation Indices. https://doi.org/10.5067/MODIS/MOD13A2.061
11. Abatzoglou, J. T. 2013. Development of gridded surface meteorological data for ecological applications and modelling. *International Journal of Climatology* 33:121–131.
12. Ketchum, D., K. Jencso, M. P. Maneta, F. Melton, M. O. Jones, and J. Huntington. 2020. IrrMapper: A machine learning approach for high resolution mapping of irrigated agriculture across the western U.S. *Remote Sensing* 12:2328.
13. Pekel, J.-F., A. Cottam, N. Gorelick, and A. S. Belward. 2016. High-resolution mapping of global surface water and its long-term changes. *Nature* 540:418–422.
14. Dewitz, J, and USGS. 2021. National land cover database (NLCD) 2019 products. U.S. Geological Survey.
15. Barton, K. 2023. MuMIn : multi-model inference. https://CRAN.R-project.org/package=MuMIn.